

Prediction of Oil Spill Trajectory on the Ocean Surface Using Mathematical Modeling

Anagha S. Dhavalikar^{ID}, *Student Member, IEEE*, and Pranali C. Choudhari

Abstract—A simplistic mathematical model based on the law of motion for predicting oil spill trajectory on the ocean surface utilizing random walk technique is proposed in this article. Validation of the proposed model is performed by comparing results with the General NOAA Operational Modeling Environment model and the available set of periodic Sentinel-1 synthetic aperture radar (SAR) images of the contingency location (Corsica oil spill incident in the Mediterranean Sea). SAR images are processed for speckle noise removal, dark spot detection, feature extraction, and classification of dark spots as oil spills and look-alikes for suitability of comparison. The accuracy of prediction is evaluated using centroid skill score metric and is compared with that of the prediction results from MEDSLIK-II model. The results of proposed model are found to be in good agreement with available SAR images. The simulation also showed that using an hourly wind and ocean current data on the study region, more accurate prediction of the trajectory is possible.

Index Terms—Centroid skill score (CSS), ocean wind and current, oil spill, random walk procedure, synthetic aperture radar (SAR), trajectory prediction.

I. INTRODUCTION

UNDRY reasons for oil spills in the ocean include daily ship traffic for oil conveyance, operations on oil rigs, contingent ship collision or sinking of oil tankers, natural oil seeps from seabed oil sources, etc. Contingent oil spills cause earnest threats through their long-term and hazardous effects on the ocean ecosystem. In case of sizably voluminous oil spill incidents, like ship collisions or explosions on oil platforms, the possibility of perpetual oil spills in the ocean is very high. The impacts of these variants of oil spills, in general, depend on the type and quantity of spilled oil, atmospheric conditions, effects on the ocean ecosystem, and sea state conditions [1]. In such situations, it is very consequential for the responsible agencies to know in advance the direction of the convey and the fate of spilled oil contaminants in the ocean so as to take expeditious clean-up actions and avert oil from spreading in the ocean. But environmental

conditions like wind, waves, and ocean currents can affect the oil spill trajectory in different ways. After an oil spill in the ocean, properties of oil such as density, viscosity, etc. are affected by the ocean currents, waves, wind, and solar radiation over some time [2]. When oil is spilled at sea, it spreads out and moves on the sea surface with wind and current while undergoing several chemical and physical changes. These processes are collectively termed weathering processes and determine the fate of oil in the ocean. A cumulation of different weathering processes like evaporation, emulsification, dispersion, etc. causes the spilled oil in the ocean to break down and spread under the influence of wind speed and direction and withal ocean currents.

Weathering processes, like spreading, evaporation, dispersion, and biodegradation, avail in minimizing some volume of oil over some time. The rate of evaporation depends on the oil's composition and many components of heavier oils will not evaporate at all, even over long periods and at high temperatures. About 80% of evaporation occurs in the first two days after a spill [3]. The remaining oil on the sea is spread by the effect of wind and sea currents' direction and velocity. Locations of these oil spills can be easily identified using remote sensing information. Synthetic aperture radar (SAR) imaging technology, due to its all-day all-weather imaging capability, has been widely used to provide an accurate positions and extent of the oil spill spread on the ocean. However, its use for tracking oil spill trajectories is limited due to satellite revisit time and the swath of the SAR. Also, distinguishing the oil spills and look-alikes (algae, rain cells, low wind areas, etc.) from SAR images is an important challenge. Hence, the use of SAR images can be combined with model simulations in order to get more accurate oil spill information especially for oil spill monitoring and tracking during significant oil spill events [4]. Recent development in the field of artificial intelligence (AI) has also attracted the remote sensing scientists. Earlier, various techniques of oil spill remote sensing with different algorithms for discrimination between oil spills and look-alikes using segmentation and deep learning have been discussed and demonstrated in [5]–[12]. Remote sensing data tend to suffer from various degradations, speckle noise effects, or variabilities in the process of imaging. Hong *et al.* [13] had proposed an augmented linear mixing model to address spectral variability for hyperspectral unmixing and had also proposed an in-depth methodology of some currently advanced AI models in remote sensing for solving image classification problems [14]–[16].

Oil remote sensing helps emergency responders to monitor an oil spill, along with changes in chemistry and mass fluxes, and

Manuscript received 27 April 2022; revised 10 June 2022; accepted 10 July 2022. Date of publication 19 July 2022; date of current version 1 August 2022. (*Corresponding author:* Anagha S. Dhavalikar.)

Anagha S. Dhavalikar is with the Electronics and Telecommunication Department, Father Conceicao Rodrigues Institute of Technology, Navi Mumbai 400703, India and also with the Electronics and Telecommunication Department, Vasantdada Patil Pratishthan's College of Engineering and Visual Arts, Mumbai 400022, India (e-mail: anaghad@pvppcoe.ac.in).

Pranali C. Choudhari is with the Electronics and Telecommunication Department, Father Conceicao Rodrigues Institute of Technology, Navi Mumbai 400703, India (e-mail: pranali.choudhari@fcrit.ac.in).

Digital Object Identifier 10.1109/JSTARS.2022.3192352

thereby to develop insights into the different physical processes for determining the fate of oil on the ocean, whether from natural or anthropogenic sources. The oil thickness and oil: water ratio was derived from remote sensing spectral data on the deepwater horizon oil spill on May 17, 2010 to identify the source of the oil spill in [17]. Oil flow modeling and remote sensing information can provide the right synergy to determine the timing and transportation of oil and obtain reliable estimates of spilled oil thickness to create a contingency plan and assess the importance of the threat in the event of an oil spill disaster [18]. Information on slick location, extent, thickness, and drift direction is critical for the response teams to combat the devastating effects of oil spills on the marine environment [19]. Combined observations from microwave and optical sensors allow the slicks to be followed during its movement [20]. Using monitoring data and numerical models together can be beneficial in understanding coastal processes, and to obtain consistent and accurate results, it is essential to run numerical models that have been previously implemented and calibrated with reliable field data [21]. New technologies and remote sensing techniques were developed in the first decade of the 21st century and used during the deepwater horizon disaster. Visible satellite sensors MODIS and MERIS actively supported the response and, to some extent, the SAR satellite [22]. In reality, the oil spill can be simulated based on Euler's equations for fluid flow. Most appropriate would be to consider Navier Stoke's equations (computational fluid dynamics), which consider the fluid viscosity as well to model turbulence and the principles of solution are the conservation of mass, momentum, and energy [23]. These are typically partial differential equations, and solution follows various numerical techniques for time and space marching and computationally intensive. Also, these techniques require sensitivity studies w. r. t. the computational mesh and time step.

The main motivation behind this article is to demonstrate the combined use of SAR imagery and model simulation for predicting the oil spill trajectory in case of accidental oil spills. In the present article, authors propose a simplistic mathematical model based on the law of motion. The article utilizes the Sentinel-1 images of observed oil spills for validation of oil spill trajectory prediction model. This model relies on the random walk technique for predicting the path of oil particles on the ocean surface and then on the comparison of the simulated trajectory with the detected oil spills in the periodic SAR images. Using the Corsica oil spill accident that happened on October 7th, 2018, as a case study, the relevance of the proposed model is demonstrated and validated in this article. The randomness in the prediction of oil trajectory is included by random walk term, which follows Gaussian distribution. It includes the horizontal dispersion terms [x and y directions only, i.e., two-dimensional (2-D) plane]. The presented mathematical model is simplistic. Validation studies indicate that the model can reliably be used for predictions of oil spill trajectories based on forecasted wind and current. The main objective of this article is to produce an operational tool to forecast the fate of an oil spill on the ocean and contribute to manage environmental crises from such pollution. The proposed model is user-friendly and easily accessible by all the responsible authorities.

II. STATE-OF-THE-ART

Consequential studies have been carried out in the past to model the movement of oil spilled on the ocean. Liu *et al.* [24] and [25] for the first time used surface oil locations inferred from satellite imagery to reinitialize the positions of virtual particles in the ensemble of trajectory models, and the particles were tracked using forecast surface currents, with new particles added to simulate the continual release of oil from the well. Abascal *et al.* [26] demonstrated the application of a stochastic Lagrangian trajectory model for oil spill modeling which could also quantify the uncertainties in trajectory simulations and define the most likely search area for possible trajectory. Cheng *et al.* [4] simulated the Shell North Sea Gannet Alpha platform oil spill contingency that occurred on August 10, 2011, utilizing General National Oceanic and Atmospheric Administration (NOAA) Operational Modeling Environment (GNOME). The simulated trajectory was found in good agreement with that observed by COSMO-SkyMed X-band SAR images. Gautama *et al.* [27] combined SAR-based oil spill detection with a Lagrangian analysis and numerical tools using wind and sea current data for the Montara oil spill incident. The model was based on wind and current related drift parameters, the origin, and the duration of oil leakage. Given an SAR-derived oil spill detection, a numerical inversion was utilized to optimize these model parameters, so that the simulated drift matched the SAR-derived optical discernment. Jeznach *et al.* [28] simulated the fate and transport of the crude oil components within a reservoir using the proactive spill modeling method to assess water quality impacts during an accidental crude oil spill. A mathematical model describing the propagation of oil slicks after an accident was proposed by [29] for the identification of pollution sources and the accident time of oil emission. There are some oil spill models that are extensively utilized at the global level to simulate the evolution of an oil spill in the ocean [30]. Most of the 2-D spreading models predicated on the Lagrangian approaches have defined the oil spreading dynamics surmising that the spilled hazardous material consists of an immensely colossal number of particles that move in water according to dispersion models [31]. Simulation of the prediction of an oil spill movement on the ocean highly depends on various physicochemical processes between the oil phase and the water column [32]. Liu and Weisberg [33] proposed a new skill score method primarily based totally at the cumulative Lagrangian separation distances normalized with the aid of using the related cumulative trajectory lengths. This skill score was used to assess surface trajectories implied with the aid of using Global HYCOM hindcast surface currents as gauged toward real satellite-tracked drifter trajectories with inside the Gulf of Mexico during the 2010 Deepwater Horizon oil spill. Dearden *et al.* [34] further proposed some performance metrics based on [33] to provide an accuracy measure of the oil spill dispersion models to simulate real-world oil spills and demonstrated how those metrics can be often used to assess the sensitivity of a model to its input parameters and their impact on the accuracy of the resultant forecast. These performance metrics can be applied to the output from both satellite imagery and coastal impact reports as the basis of the validation.

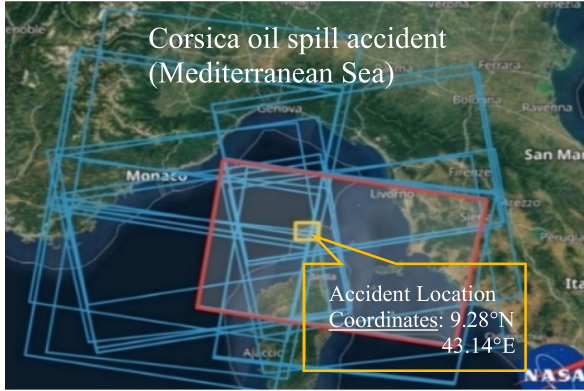


Fig. 1. Copernicus Sentinel data [2018]. Retrieved from ASF DAAC [10/08/18, 05:27:57], processed by ESA [36].

In this article, a mathematical model for the trajectory forecast of oil spills on the ocean surface has been developed and simulated utilizing the random walk procedure. The proposed model is predicated on the simple law of motion, i.e., Distance = Velocity \times Time. The model is tested utilizing the Corsica oil spill contingency in the Mediterranean Sea. The simulation results are validated with the results of GNOME simulation and the available periodic Sentinel-1 SAR images of the oil spill incident. Accuracy of prediction by the proposed model is evaluated by computing an error between the centroids of predicted and observed trajectory paths that are found to be in good agreement. In the existing and publicly available GNOME model, user has to manually enter each input parameter, which is a tedious and time-consuming task. Also, the simulation results are available only in terms of visual animation file. The main advantage of the proposed model over the existing models is that the user needs a single data file (excel/CSV) containing all input parameters to run the model instead of entering each individual parameter. Also, for an hourly input wind and sea current information, the proposed model can produce an output excel/CSV file with hourly Lat–Lon positions of the oil particles spread predicted for the given period of simulation. These predicted Lat–Lon positions can be used by the responders to start with immediate clean-up actions.

III. SELECTED STUDY AREA

For testing the proposed oil spill trajectory forecast model, Corsica oil spill incident has been selected for simulation and validation as shown in Fig. 1. The model is simulated utilizing the Corsica oil spill contingency happened due to a ship collision on October 7th, 2018 at 6:30 am, UTC in the Mediterranean Sea. This oil spill incident resulted in approximately 600 m³ of fuel oil spills in the ocean [35]. Available periodic Sentinel-1 images of the selected study region are utilized for validation of simulation.

IV. PROPOSED METHODOLOGY FOR OIL SPILL FORECAST

Advection of an oil spill on the ocean surface is computed as a simple vectorial weighted sum of the wind velocity and

the depth-averaged current velocity by most of the oil spill models [37]. This wind-drift factor approach is based on the two assumptions: 1) since the effects of wind and flow on the surface accident act independently, it can be explained as the vector sum of velocities; and 2) the outflow velocity due to the wind is a small part of the wind velocity. The direction of oil spill movement is a nonzero angle (called a deflection angle) with respect to the wind direction due to the Coriolis force [37]. Parameterization of wind induced oil spill transport with fixed and variable deflection angles has been discussed and demonstrated in detail in [37] and [38]. Reed *et al.* [39] presented and tested oil spill model with four experimental oil spills in 1989 and 1991. It was observed that oils forming stable and viscous emulsions will be drifted majorly by the wind forcing, while that do not form emulsions will be drifted majorly by current.

The proposed oil spill trajectory forecast model is based on horizontal displacement (spread) of particles/parcels using random walk procedure under the cumulated action of wind and ocean current. The total volume of the oil spilled on the sea surface is characterized under the influence of the regular movement of the media with velocity components u and v . Velocity components are determined by the dynamical field resulting in Kelvin wave for each time interval [40]. A single input file (excel/CSV) with the input parameters like type of oil, the quantity of oil spilled, duration of simulation, wind speed, wind direction, also the speed and direction of ocean currents are used. The oil spill model for the selected region of interest is simulated in a MATLAB environment utilizing a world ocean shapefile. The model generates 10 random points on the oil spill origin location. These points represent oil spill particles/parcels in the ocean. The random points follow Gaussian distribution. i.e., mean (μ) = 0 and std. deviation (σ^2) = 1. Collection of these 10 particles at origin represents the initial status of oil spill, i.e., X_k^0 and Y_k^0 . Boundary condition for discriminating land and ocean area is set so that the spread of oil will stop on the shoreline exhibiting the oil beaching. In this article, sea surface wind and ocean current data are acquired from Copernicus Climate Data Store, European Centre for Medium Range Weather Forecast (ECMWF) [41], and NOAA-developed GNOME Online Oceanographic Data Server (GOODS) [42], [43], respectively, with 1 h temporal resolution. Wind speed (U_w), at 10 m above sea level, obtained from the ECMWF reanalysis dataset is used. However, the entire wind force does not act on each oil particle, hence only some percent of wind speed (windage) is considered. A total of 5% windage [(3) and (4)] is arrived at with trial and error and comparing with the available data. Velocity components of wind and ocean current in x and y directions are given as follows:

$$u_1 = U_w * \sin(\theta_w * \pi / 180) + U_c * \sin(\theta_c * \pi / 180) \quad (1)$$

$$v_1 = U_w * \cos(\theta_w * \pi / 180) + U_c * \cos(\theta_c * \pi / 180). \quad (2)$$

Velocity components of oil particles with respect to that of wind and ocean current in x and y directions are given as follows:

$$u = 5/100 * U_w * \sin(\theta_w * \pi / 180) + U_c * \sin(\theta_c * \pi / 180) \quad (3)$$

$$v = 5/100 * U_w * \cos(\theta_w * \pi / 180) + U_c * \cos(\theta_c * \pi / 180) \quad (4)$$

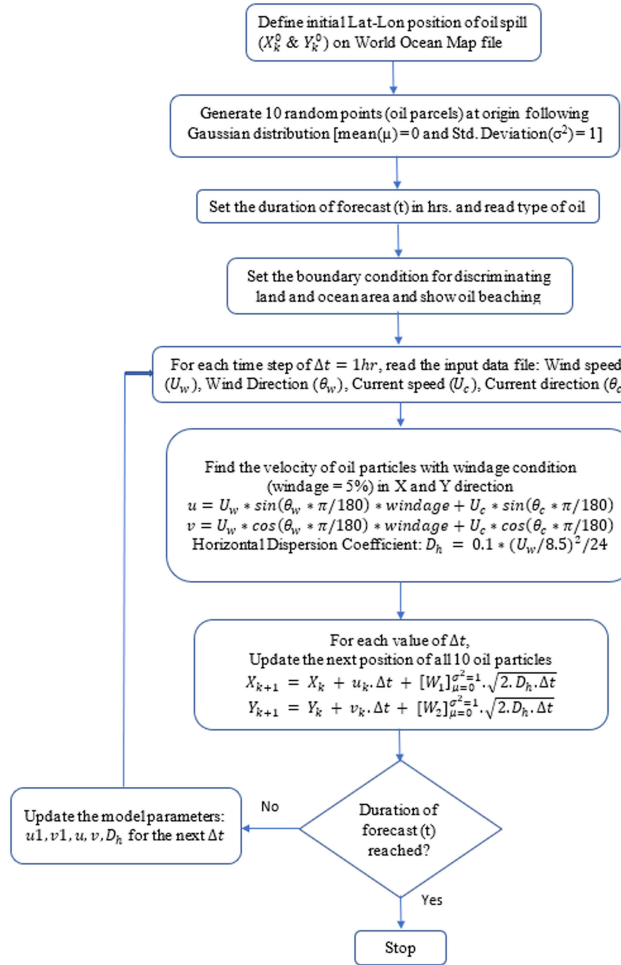


Fig. 2. Basic steps in simulation model for oil spill trajectory path forecast.

where U_w and U_c represent wind speed and ocean current speed in m/s, respectively, while θ_w and θ_c are wind and ocean current direction w. r. t. north in degrees, respectively. New position of oil particles on the ocean surface is predicted by random walk procedure over the period of time Δt [40] as follows:

$$X_k = X_{k-1} + u_k \cdot \Delta t + [W_1]_{\mu=0}^{\sigma^2=1} \cdot \sqrt{2.D_h.\Delta t} \quad (5)$$

$$Y_k = Y_{k-1} + v_k \cdot \Delta t + [W_2]_{\mu=0}^{\sigma^2=1} \cdot \sqrt{2.D_h.\Delta t} \quad (6)$$

where X_k and Y_k are the coordinates of the new position of parcels (oil particles) at time (t). X_{k-1} and Y_{k-1} are the coordinates of the previous position of parcels (oil particles) at time ($t-1$), and u_k and v_k represent velocity of oil particles in x and y directions, respectively. W_1 and W_2 are random particles/parcels with mean zero and variance one

$$D_h = 0.1 * (U_w/8.5)^2/24. \quad (7)$$

D_h is the horizontal dispersion coefficient, which governs the spread of oil over the time [32] given by (7). Beyond certain period, say more than 24 h, it is likely that dispersion will reduce. This can be investigated by making D_h as a function of time. Presently, it is assumed that D_h is independent of time. Fig. 2

shows the sequence of important steps for model simulation for a set duration of forecast. Random walk model is one of the simplest and most important models in time series forecasting. This model is based on the assumption that in each period the variable (in this case, oil parcel) takes a random step away from its previous value, and the steps are independently and identically distributed in size [44]. Equations (5) and (6) are derived from the state space model (SSM) representation. The SSM is identical to a hidden Markov model, but the variables in SSM follow continuous Gaussian distributions and this property can be used to derive SSM [45]. Consider a particle moving in 2-D space. The new trajectory position, X_k , is determined by the old position (X_{k-1}) and velocity of the particles according to the Newton's law of motion. Thus, X is the latent variable sequence corresponding to the path and is given by

$$\text{New position} = \text{Old position} + \Delta t \cdot (\text{old velocity}) + \text{noise}$$

where noise represents the randomness added at each time instant due to a random movement of particles/parcels. Since the new position is a linear combination of the old position and the velocity, in practice, SSM can be applied to track the trajectory of particles in a 2-D plane. Thus, an SSM for predicting the path of oil particles on the ocean surface can be derived from (5) and (6) as follows:

$$\begin{bmatrix} X_k \\ Y_k \end{bmatrix} = \begin{bmatrix} 1 & 0 \\ 0 & 1 \end{bmatrix} \begin{bmatrix} X_{k-1} \\ Y_{k-1} \end{bmatrix} + \begin{bmatrix} u_k & 0 \\ 0 & v_k \end{bmatrix} \Delta t + \begin{bmatrix} W_1 \\ W_2 \end{bmatrix} \sqrt{2.D_h.\Delta t}. \quad (8)$$

Equation (8) gives the SSM representation for predicting the new position (X_k , Y_k) of oil particles on the ocean surface from the previous position (X_{k-1} , Y_{k-1}). W_1 and W_2 are the random vectors in x and y directions, respectively, at each time instance. Thus, random walk technique is a simple and easy-to-implement method to predict the movement of complex oil spills on the ocean surface. Random walk method is best suited for predicting probable locations of random points independent of the previous locations.

A. Evaporation of Oil

After an oil spill event, an immediate weathering process affecting the oil quantity on the ocean surface is evaporation before it forms water-in-oil emulsions. The process of evaporation differs fundamentally for a pure liquid such as water and a multicomponent system such as crude oil [46]. For crude oils and other multicomponent fuel mixtures, loss in weight or volume due to evaporation is not linear with time [47]. Evaporation of oil on the ocean surface is not air-boundary-layer regulated and is also independent of wind velocity, turbulence level, area, and scale size. The consequential factors responsible for the evaporation of oil include time and temperature. Oils and fuels evaporate either as a logarithm of time or as a square root of time. Fingas [47] has given evaporation equations for various types of oils and fuels, some of which, considered here for oil spill trajectory mapping, are given in Table I. In the given equations, T and t represent the temperature and time, respectively.

TABLE I
EQUATIONS FOR DIFFERENT OIL EVAPORATION [47]

Sr. No.	Oil type	Evaporation Equations
1	Jet Fuel short term	$\% Ev = (1.06 + 0.013 T) \cdot \sqrt{t}$
2	Diesel Fuel 2002 short	$\% Ev = (0.39 + 0.013 T) \cdot \sqrt{t}$
3	Fuel oil #5	$\% Ev = (-0.14 + 0.013 T) \cdot \sqrt{t}$
4	IFO-300 (old Bunker C)	$\% Ev = (-0.15 + 0.013 T) \cdot \sqrt{t}$
5	Gasoline	$\% Ev = (13.2 + 0.21 T) \cdot \ln(t)$
6	IFO-30 (Svalbard)	$\% Ev = (-0.04 + 0.045 T) \cdot \ln(t)$

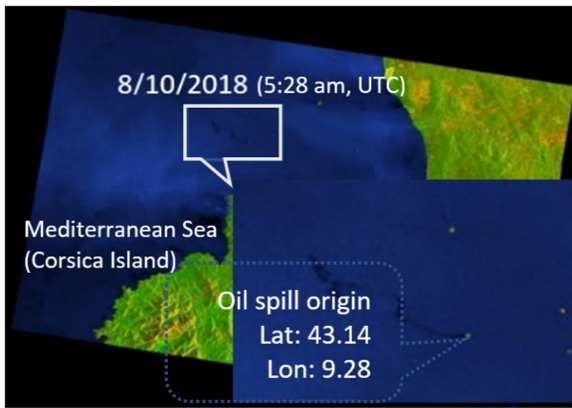


Fig. 3. Copernicus Sentinel data [2018]. Retrieved from ASF DAAC and processed by ESA [36].

V. RESULTS AND DISCUSSION

A. Oil Spill Scenario (*Corsica Oil Spill, Mediterranean Sea*)

The proposed model is tested using the Corsica oil spill accident that occurred due to a collision between two ships in the Mediterranean Sea on October 7th, 2018, which resulted in a release of about 600 m^3 of oil in the ocean [35], [48]. On October 8th, 2018 at 05:28 am (UTC), the first image of the oil spill from this collision was acquired by the Copernicus Sentinel-1A satellite as shown in Fig. 3.

Following is the summary of the oil spill incident as per the literature reports [31], [35], and [48]:

- 1) Date of collision resulting in oil spill: October 7th, 2018, 6:30 am, UTC.
- 2) First Sentinel-1 image of oil spill location: October 8th, 2018, 5:28 am, UTC (length = 20 km)—Fig. 4(a).
- 3) Second Sentinel-1 image of oil spill location: October 8th, 2018, 5:21 pm, UTC (length = 35 km)—Fig. 4(b).
- 4) Third Sentinel-1 image of oil spill location: October 9th, 2018, 5:14 pm, UTC (length = 60 km)—Fig. 4(c).
- 5) Fourth Sentinel-1 image of the spill location: October 14th, 2018, 5:27 am, UTC—Fig. 4(d).
- 6) Approximately 14% of the oil had been evaporated, ~75% had been dispersed, ~2% had been washed ashore, and ~9% had been still at the sea surface till October 16th, 2018 [48].
- 7) Sentinel-1 image of the Saint Tropez Beach: October 20th, 2018, 5:21 pm, UTC (showing oil beaching)—Fig. 5(a)

- 8) Sentinel-1 image of the Saint Tropez Beach: October 24th, 2018, 5:43 am, UTC (showing oil beaching)—Fig. 5(b).

Fig. 4(d) shows the Sentinel-1 image of the nearby contingency location acquired on October 14th, 2018 at 5:27 am, UTC. As depicted in the image, some long, thin, and broken oil slicks were visually perceived floating near the initial path which was followed by the oil spill trajectory in the first 24 h.

1) Wind and Ocean Current Data Used for Prediction: The proposed simulation model reads the input parameters from a CSV or excel file. The horizontal displacement of Lagrangian particles is conditioned in the direction and speed by the vectorial sum of 5% of the input wind speed and sea current. The model is applied to simulate the oil spill forecast trajectory for 14 days from October 7th to October 20th, 2018. Wind speed over the ocean surface during October 7th to October 25th ranged between 3.6 m/s and maximum 12.77 m/s as shown in Fig. 6(a). The oil spill trajectory is initially directed in the North-West direction for the first three days till October 9th, 2018. Later with the change in wind and sea current direction, it is directed toward East and then South-West moving toward the Saint Tropez beach [31].

Due to very high wind speed conditions in the first few days after the incident, the responsible authorities could not reach the accident spot. As a result, there was a continuous oil discharge from the ship till October 11th, 2018 when the two ships were separated [48]. Ocean current information for the selected region is acquired from the NOAA-developed GOODS [43] that helps to access publicly available base maps, ocean currents, and wind information for the selected region of interest as depicted in Fig. 6(b). GOODS offers currents from global and regional ocean current models, as well as measured currents from several sources. The average ocean current speed from October 7th to October 25th ranged from -0.2 to 0.3 m/s as depicted in the Fig. 7.

B. Prediction Based on Random Walk Procedure

Fig. 8 depicts the results of oil spill trajectory forecast simulated for 23 h, 35 h, 59 h, and 14 days. Black particles indicate the simulated trajectory forecast, while particles in red color show the oil parcels at the last instant. Corresponding simulation videos for Fig. 8(c) and (d) can be found on the links provided with the respective figure caption. Particles marked in red and “+” indicate the oil beaching as depicted in Fig. 8(d). The direction and extent of oil spill spread on the ocean is governed by the hourly input wind and sea current speed and direction for the period of simulation.

1) Evaporation Calculations: Evaporation is not included in the oil spill trajectory presage. However, Fig. 9 shows the hourly evaporation of oil that can be calculated utilizing the equations as per Table I considering oil type as Fuel oil#5. Approximately 14% of the oil had been evaporated, ~75% had been dispersed, ~2% had been washed ashore, and ~9% had been still at the sea surface till October 16th, 2018 as reported in [48]. Table II gives the comparison of spilled oil quantity till October 16th (10 days) from the available literature and that derived from the proposed model simulation. From Fig. 9, percent of oil evaporated for

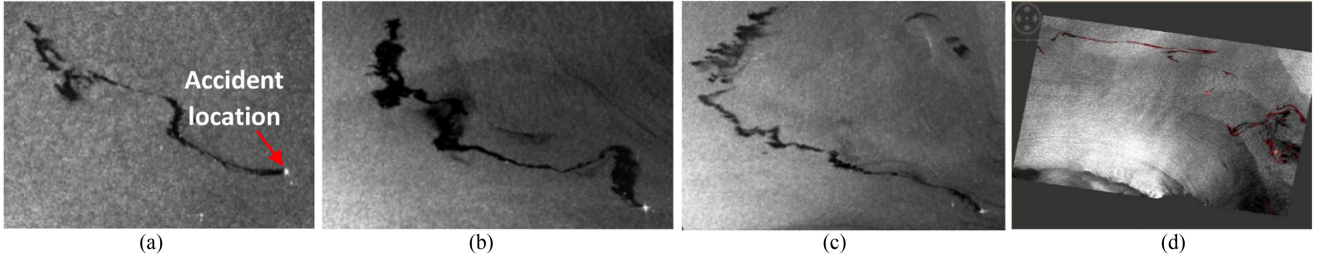


Fig. 4. Gradual increase in the oil slick length near accident location: (a) 1st Sentinel-1 image dated 8/10/2018 (5:28 am UTC); (b) 2nd Sentinel-1 image dated October 8th, 2018 (5:21 pm UTC); (c) 3rd Sentinel-1 image dated October 9th, 2018 (5:14 pm UTC); and (d) 4th Sentinel-1 image dated October 14th, 2018 (5:27 am UTC).

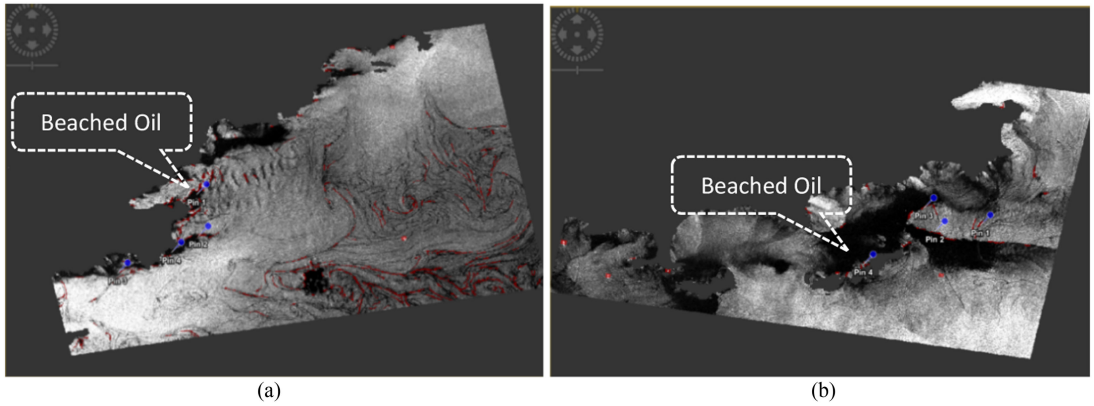


Fig. 5. SAR image with oil spill mask (in red) near Saint Tropez coastline [36]: (a) October 20th, 2018, 5:21 pm, UTC; and (b) October 24th, 2018, 5:43 am, UTC.

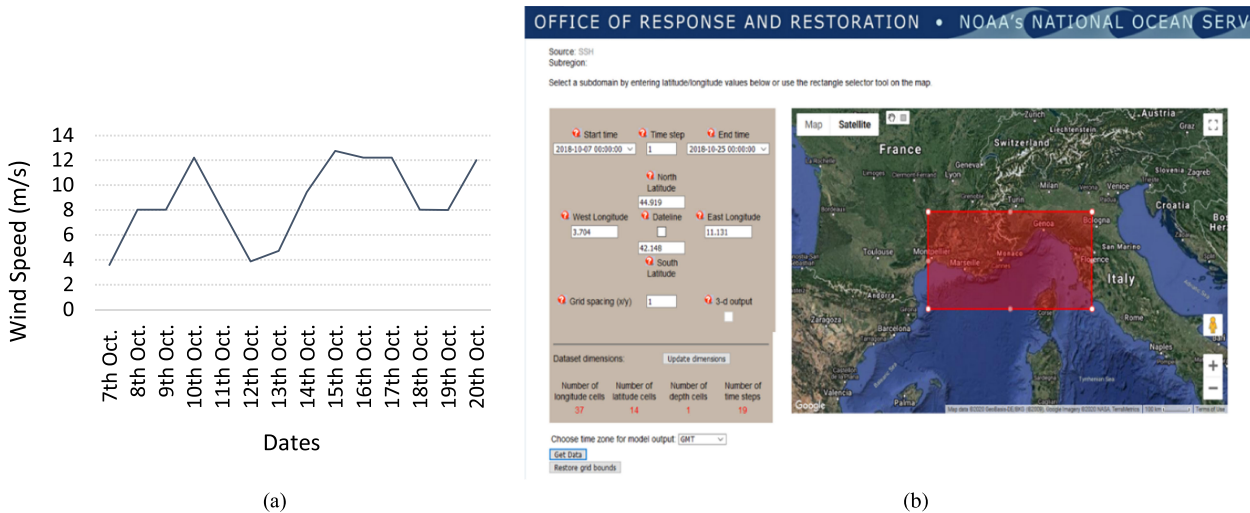


Fig. 6. (a) Average wind speed near the accident location. (b) Ocean current data for selected period and region of interest [43].

TABLE II
COMPARISON OF SPILLED OIL QUANTITY TILL OCTOBER 16TH (10 DAYS)

Status of spilled oil till 16 th Oct. 2018	Spilled oil status as per Ref. [48] (Up to 10 days)	Spilled oil status as per proposed model simulation (10 days)
Oil Evaporated	~ 14 %	14.4 %
Floating oil and beached oil	~ 11 %	20 %
Oil Dispersed	~ 75 %	65.6 %

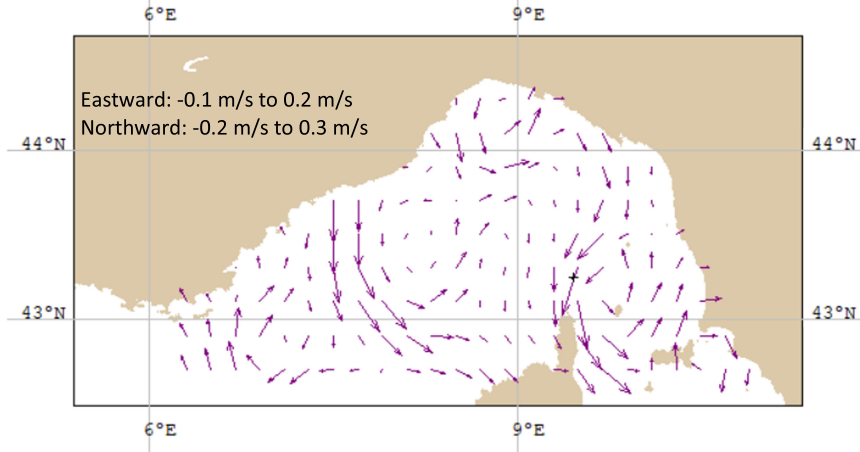


Fig. 7. Ocean current in the region of interest from October 7th to October 25th, 2018.

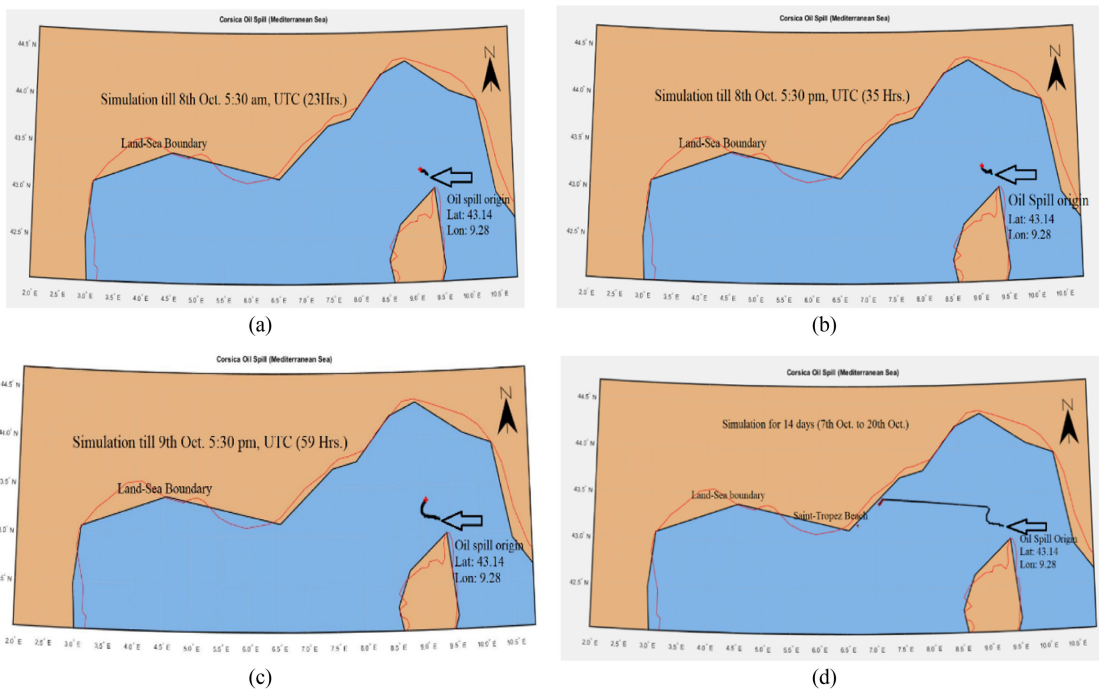


Fig. 8. Simulation model for trajectory forecast run for (a) 23 h, (b) 35 h, (c) 59 h, and (d) for 14 days.¹

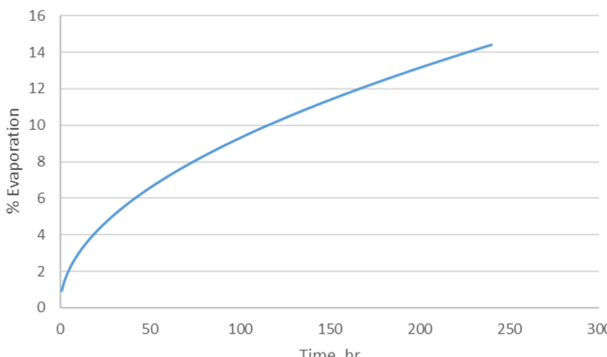


Fig. 9. Hourly evaporation prediction of oil.

240 h (10 days) till October 16th is 14.4%. The predictions consider the beaching of oil as shown in Fig. 8(d). In the present simulation, initially oil spill is modeled utilizing 10 particles. It is visually examined that only two particles remain floating on the sea surface at the cessation of 10 days' simulation. It designates that 20% of oil was floating on the sea surface which is in fair agreement with the available data as described in [48].

2) *Effect of Dispersion Coefficient:* Performance of wind numerical data and observed HF radar currents demonstrated

¹[Online]. Available: <https://drive.google.com/file/d/1YpyImHugF66ujBsVikT6zf8SOYgmnrD/view?usp=sharing> https://drive.google.com/file/d/132KIBAqRZfPPiBoijXVH46q7WL8I_Hk/view?usp=sharing

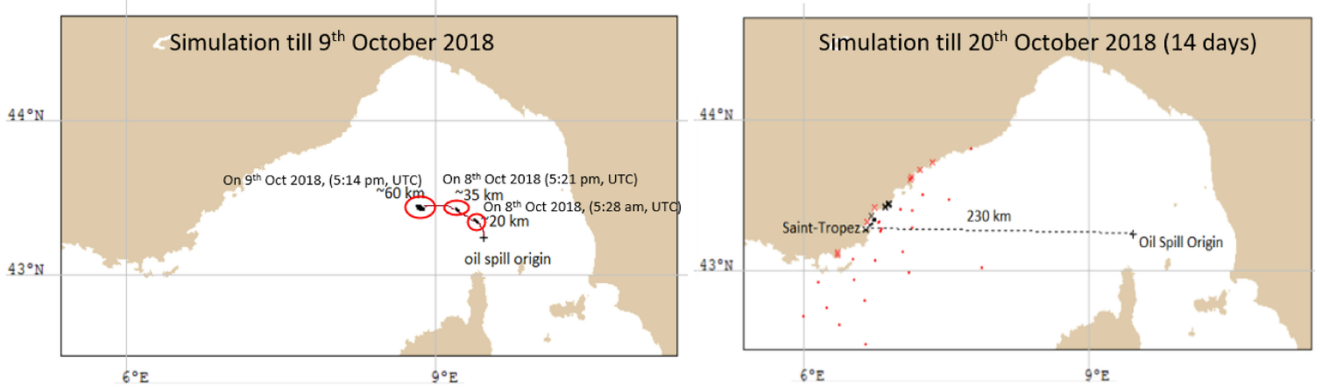


Fig. 10. GNOME Simulation run for 23, 35, and 59 h and 14 days.

a better performance of a buoy trajectory simulation compared to that with only wind numerical data as discussed in [49]. The direction of the waves may facilitate the transport of oil to the beach rather than the direction of the circulation. Circulation brings oil closer to the beach, while the waves of stokes drift actually calm the oil. A combination of observations and numerical model simulations is used to demonstrate this in [50].

The result of wind on ocean surface is creation of waves and swell (waves travelled to another location due to wind) that are important in oil spill trajectory mapping. Natural dispersion occurs when fine droplets of oil are transferred into the water column by wave action or turbulence and it can be insignificant or temporarily displace some of the oil depending on oil conditions and the amount of sea energy available [33]. It is also suggested that natural dispersion should not be included in oil spill model, as such inclusion can be misleading as natural dispersion has not been quantitatively measured in actual spill [33]. In the present article, authors considered only horizontal movements of oil particles with the consideration of dispersion coefficients in horizontal plane only and dispersion coefficient in z -direction is discarded. Including z -direction, dispersion will account for wave effect to a smaller extent, however it needs further investigation. These effects are important to investigate the environmental effects on oil, i.e., emulsification, evaporation, etc., which is beyond the present scope of article. Equation (7) for horizontal oil dispersion coefficient (D_h) is considered from literature [32]. From (7), it can be noted that D_h is of the order of $5e-5$ to $5e-3$ for the wind velocity of 1 to 10 m/s.

3) *Computation of Spill Lengths Using GNOME:* NOAA predicts spill spread utilizing an NOAA-developed computer model called GNOME, which avails to presage the movement of oil [51]. GNOME is an oil spill trajectory modeling software that is available for public use. Ocean current, wind information, geocoordinates of the oil spill inception, and the quantity of oil spill are important input parameters in GNOME required to engender an oil spill trajectory model. During Corsica oil spill incident, the floating oil on the ocean surface, travelled toward the coasts in the South-West direction and affected many coastlines due to wind speed and direction [31], [48]. Using the same input parameters used for the proposed model, Corsica oil spill incident is also simulated in GNOME. Fig. 10 depicts the

distance covered by the oil spills in 23, 35, and 59 h, and the beaching of oil spill after 14 days, i.e., on October 20th, 2018.

4) *Comparison of Predicted Trajectory With SAR Images:* The available Sentinel-1 images of the oil spill location dated October 8th, October 9th, October 14th, October 20th, and October 24th, 2018 helped validating the proposed model to map the area affected by the pollution. The subset scenes of the accident location from SAR images are initially preprocessed for speckle noise removal using Gaussian filter. The oil spill detection from input SAR images is done using a three-step procedure: 1) dark spot detection using adaptive thresholding, 2) feature extraction, and 3) classification of dark spots as oil spills and look-alikes. For an accurate discrimination between oil spills and look-alikes bag of visual words method of feature extraction and classification is used as proposed in [52]. Geolocation coordinates of all the available oil spill scenes from SAR images are then compared with that of the simulated model. Comparison between the forecasted oil slick path and Sentinel-1A satellite images in Fig. 11 shows a fairly good agreement, with a prevailing direction of the oil slicks.

Table III shows the comparison of geolocation coordinates of the oil spill spread after 23, 35, 59 h, and 14 days in GNOME, SAR images, and the trajectory predicted from the forecast model, while Table IV gives the comparison of distance travelled by the oil slicks at different time intervals using QGIS (measured from SAR images), GNOME, and the proposed simulation model.

5) *Accuracy Assessment of the Proposed Model:* Accuracy of prediction by the proposed model is evaluated by adopting the centroid skill score (CSS) as one of the evaluation metrics following the pioneering work in [33] and [34]. The CSS helps to identify how close the predicted trajectory is to the observed oil spill in the SAR images. For calculating the CSS, initially a centroid displacement index C_I is computed as given as

$$C_I = \Delta_x / L_{\text{OBS}} \quad (9)$$

where Δ_x is the distance between the geometric centers (centroids) of the observed oil spill shape in the SAR image and the predicted oil spill shape at a given time instance, and L_{OBS} is the length scale of the observed oil spill area, which is defined as the distance along the diagonal of a bounding box enclosing the

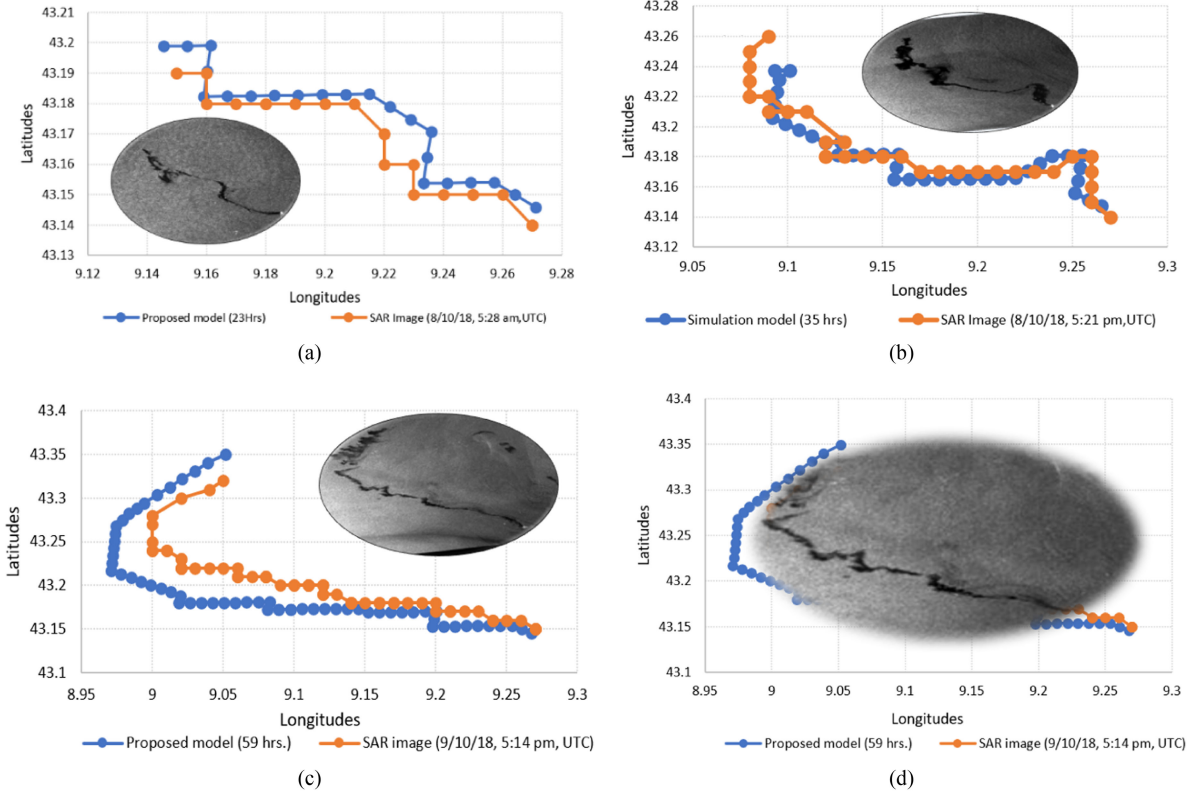


Fig. 11. Comparison of simulated Lat–Lon with SAR image Lat–Lon (a) dated October 8th, 2018; 5:28 am, UTC; (b) dated October 8th, 2018; 5:21 pm, UTC; (c) dated October 9th, 2018; 5:14 pm, UTC; and (d) comparison of simulated Lat–Lon with overlapped SAR image.

TABLE III
COMPARISON OF OIL SPILL SPREAD LAT–LON COORDINATES

Sr. No.	Simulation period	GNOME (Lat–Lon)	SAR Images (Lat–Lon)	Proposed Model (Lat–Lon)
1	23 Hrs.	Lat: 43.20, Lon: 9.18	Lat: 43.21, Lon: 9.14	Lat: 43.26, Lon: 9.12
2	35 Hrs.	Lat: 43.24, Lon: 9.10	Lat: 43.26, Lon: 9.09	Lat: 43.40, Lon: 8.87
3	59 Hrs.	Lat: 43.26, Lon: 8.53	Lat: 43.32, Lon: 9.05	Lat: 43.46, Lon: 8.41
4	14 days	Lat: 43.17, Lon: 6.40	Lat: 43.12, Lon: 6.41	Lat: 43.13, Lon: 6.70

TABLE IV
COMPARISON OF DISTANCE COVERED BY OIL SPILL SPREAD

Date of oil spill Image	Distance covered by oil spill as per [48]	Measured length from GNOME (km)	Measured length from SAR image (km)	Calculated length from simulation (km)
8/10/2018 (5:28 am UTC)	20 km	20.3	22.544	14.904
8/10/2018 (5:21 pm UTC)	35 km	38.8	37.772	22.680
9/10/2018 (5:14 pm UTC)	60 km	64.8	60.993	40.224
20/10/2018 (5:21 pm UTC)	231 km	230	--	236.725

observed oil spill region. Thus, C_I is simply a measure of the absolute error in the predicted centroid location, normalized by the length scale of the observed oil spill. Then, CSS is defined as

$$\text{CSS} = 1 - \frac{C_I}{C_{\text{thr}}}, \text{ for } C_I < C_{\text{thr}}$$

$$\text{CSS} = 0, \quad \text{for } C_I > C_{\text{thr}}$$

where C_{thr} is a user-selected tolerance threshold and is taken to be 1 in this case. A C_{thr} value of 1 indicates that distance

between the locations of the observed and predicted centroids must not exceed the magnitude of the observed length scale [34]. Fig. 12 provides an illustration of the quantities involved in the calculation of CSS for the predicted trajectories and their corresponding periodic SAR scenes of the accident location. The CSS provides the most useful performance metric as the predicted center of the slick can be used by the responders to head toward when trying to initially locate an oil spill.

Table V gives the comparison of CSS calculated for proposed model and that calculated for the prediction done using MEDSLIK-II model in [34]. The proposed model based on

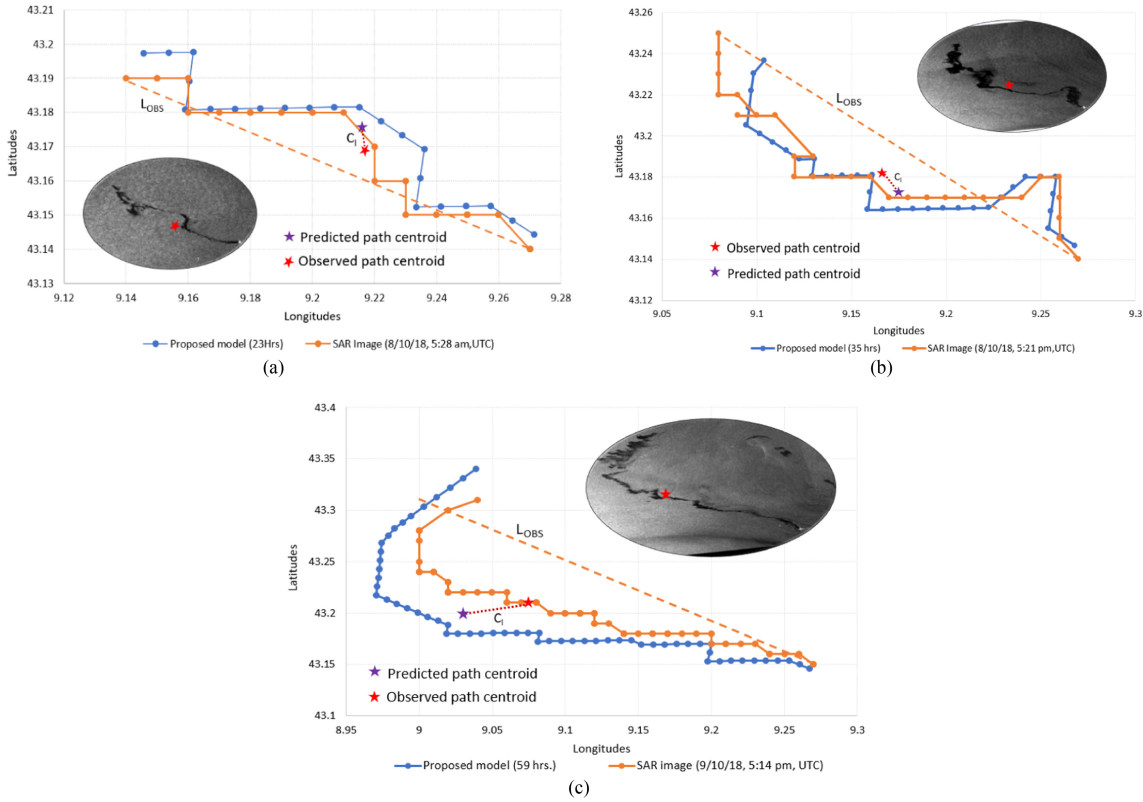


Fig. 12. Comparison of centroid distance between the predicted trajectory and the observed SAR images dated (a) October 8th, 2018; 5:28 am, UTC; (b) October 8th, 2018; 5:21 pm, UTC; and (c) October 9th, 2018; 5:14 pm, UTC.

TABLE V
COMPARISON OF EVALUATION METRICS FOR VALIDATION

Observed SAR Images	Distance between Centroids (Δ_x) in km	Observed length (L_{OBS}) in km	Centroid Index, (C_1) (Δ_x / L_{OBS})	Centroid Skill Score (CSS)	
				CSS as per Ref [34]	CSS (1- C_1) [Proposed Model]
8/10/2018 (5:28 am UTC)	0.6531	11.92	0.0547	0.81	0.94
8/10/2018 (5:21 pm UTC)	0.9270	19.67	0.0471	0.85	0.95
9/10/2018 (5:14 pm UTC)	3.605	28.2	0.1278	0.75	0.87

random walk technique is run for forecasting oil spill trajectory path using an hourly wind and ocean current data on the selected study area. It is observed that the CSS of prediction done with the proposed model is close to 1 indicating an improved prediction accuracy as compared to the results of [34]. The distance between the centroids of the predicted and observed trajectory path ranges from 0.6531 km to maximum 3.605 km for the first 3 days. This difference is acceptable, as an error between 7 and 19 km can allow the use of the model forecasts in situations of rapid response, such as oil spills and search and rescue operations [53].

VI. CONCLUSION

A mathematical model for the trajectory forecast of oil spills on the ocean surface has been proposed and simulated utilizing the random walk procedure. This model is predicated on the simple law of motion, i.e., distance given by the product of

velocity and time. The movement of oil particles on the ocean surface is majorly influenced by the speed and direction of wind and ocean current. Hence, in the proposed model, currently, only these parameters are considered to investigate the movement of oil particles in the horizontal plane on the ocean surface taking into consideration the horizontal dispersion coefficient (D_h). However, the effect of D_h on the oil particles' motion is found to be negligible after certain period. Evaporation of oil over time is predicted based on the standard exponential relations as available in the literature. The proposed model predicts the oil spill trajectory, beaching of oil, and the oil remaining on the ocean surface at the cessation of the given simulation time with reasonably good accuracy. For evaluating the accuracy of model, CSS performance metric is computed, which demonstrated that the difference or error between predicted path centroid and observed path centroid is in the acceptable range where the response agencies can reach fast. Thus, overall predictions can

be considered valid for a range of the distance, which can be covered by oil and will be serviceable for the responsible agencies to take a call-in advance. Further investigations will be required to include the effect of waves and other weathering effects like evaporation, emulsification on the movement of oil particles in the vertical direction which is not considered in the present article.

ACKNOWLEDGMENT

The authors would like to thank Mr. Sharad Dhavalikar, Principal Surveyor, Indian Register of Shipping, for discussions and technical guidance on Ocean Engineering related aspects.

REFERENCES

- [1] Statistics—ITOPF, Jan. 2021. Accessed: Jul. 26, 2021. [Online]. Available: <https://www.itopf.org/knowledge-resources/data-statistics/statistics/>
- [2] M. Fingas, “Introduction to spill modeling,” in *Oil Spill Science and Technology*, 2nd ed. Amsterdam, The Netherlands; New York, NY, USA: Elsevier, Nov. 2016, ch. 8, pp. 419–453.
- [3] A. Zafirakou, “Oil spill dispersion forecasting models,” in *Book Monitoring of Marine Pollution*. London, U.K.: IntechOpen, 2018, doi: [10.5772/intechopen.81764](https://doi.org/10.5772/intechopen.81764).
- [4] Y. Cheng *et al.*, “Monitoring of oil spill trajectories with COSMO-SkyMed X-Band SAR images and model simulation,” *IEEE J. Sel. Topics Appl. Earth Observ. Remote Sens.*, vol. 7, no. 7, pp. 2895–2901, Jul. 2014, doi: [10.1109/JSTARS.2014.2341574](https://doi.org/10.1109/JSTARS.2014.2341574).
- [5] G. A. Raeisi and A. Mahmoudi, “Combined method of an efficient cuckoo search algorithm and nonnegative matrix factorization of different zernike moment features for discrimination between oil spills and lookalikes in SAR images,” *IEEE J. Sel. Topics Appl. Earth Observ. Remote Sens.*, vol. 11, no. 11, pp. 4193–4205, Nov. 2018, doi: [10.1109/JSTARS.2018.2841503](https://doi.org/10.1109/JSTARS.2018.2841503).
- [6] A. Raeisi, G. Akbarizadeh, and A. Mahmoudi, “A new algorithm for oil spill detection from SAR images,” in *Proc. 2nd Int. Conf. Modern Mar. Technol.*, Jan. 2016.
- [7] N. Aghaei, G. Akbarizadeh, and A. Kosarian, “An accurate oil spill detection method based on level set method from synthetic aperture radar imagery,” *Eur. J. Remote Sens.*, vol. 55, 2022, doi: [10.1080/22797254.2022.2037468](https://doi.org/10.1080/22797254.2022.2037468).
- [8] P. Kolokoussis and V. Karathanassi, “Oil spill detection and mapping using sentinel-2 imagery,” *J. Mar. Sci. Eng.*, vol. 6, no. 1, Jan. 2018, Art. no. 4, doi: [10.3390/jmse6010004](https://doi.org/10.3390/jmse6010004).
- [9] X. Zhu, Y. Li, H. Feng, B. Liu, and J. Xu, “Oil spill detection method using X-band marine radar imagery,” *J. Appl. Remote Sens.*, vol. 9, no. 1, Nov. 2015, Art. no. 095985, doi: [10.1117/1.JRS.9.095985](https://doi.org/10.1117/1.JRS.9.095985).
- [10] G. Akbarizadeh and M. Rahmani, “A new ensemble clustering method for PolSAR image segmentation,” in *Proc. 7th Conf. Inf. Knowl. Technol.*, 2015, pp. 1–4, doi: [10.1109/IKT.2015.7288775](https://doi.org/10.1109/IKT.2015.7288775).
- [11] R. Garg *et al.*, “Semantic segmentation of PolSAR image data using advanced deep learning model,” *Sci. Rep.*, vol. 11, 2021, Art. no. 15365, doi: [10.1038/s41598-021-94422-y](https://doi.org/10.1038/s41598-021-94422-y).
- [12] H. Bi, F. Xu, Z. Wei, Y. Xue, and Z. Xu, “An active deep learning approach for minimally supervised PolSAR image classification,” *IEEE Trans. Geosci. Remote Sens.*, vol. 57, no. 11, pp. 9378–9395, Nov. 2019, doi: [10.1109/TGRS.2019.2926434](https://doi.org/10.1109/TGRS.2019.2926434).
- [13] D. Hong, N. Yokoya, J. Chanussot, and X. X. Zhu, “An augmented linear mixing model to address spectral variability for hyperspectral unmixing,” *IEEE Trans. Image Process.*, vol. 28, no. 4, pp. 1923–1938, Apr. 2019, doi: [10.1109/TIP.2018.2878958](https://doi.org/10.1109/TIP.2018.2878958).
- [14] D. Hong *et al.*, “More diverse means better: Multimodal deep learning meets remote-sensing imagery classification,” *IEEE Trans. Geosci. Remote Sens.*, vol. 59, no. 5, pp. 4340–4354, May 2021, doi: [10.1109/TGRS.2020.3016820](https://doi.org/10.1109/TGRS.2020.3016820).
- [15] D. Hong, L. Gao, J. Yao, B. Zhang, A. Plaza, and J. Chanussot, “Graph convolutional networks for hyperspectral image classification,” *IEEE Trans. Geosci. Remote Sens.*, vol. 59, no. 7, pp. 5966–5978, Jul. 2021, doi: [10.1109/TGRS.2020.3015157](https://doi.org/10.1109/TGRS.2020.3015157).
- [16] D. Hong *et al.*, “Spectral former: Rethinking hyperspectral image classification with transformers,” *IEEE Trans. Geosci. Remote Sens.*, vol. 60, 2022, Art. no. 5518615, doi: [10.1109/TGRS.2021.3130716](https://doi.org/10.1109/TGRS.2021.3130716).
- [17] R. N. Clark *et al.*, “A method for quantitative mapping of thick oil spills using imaging spectroscopy,” *US Geological Survey Open-File Rep.*, 2010, vol. 1167, pp. 1–51.
- [18] M. M. De P. Diana, A. Maria, and P. G. De C. Giacomo, “Synergistic use of an oil drift model and remote sensing observations for oil spill monitoring,” *Environ. Sci. Pollut. Res. Int.*, vol. 24, pp. 5530–5543, 2017, doi: [10.1007/s11356-016-8214-8](https://doi.org/10.1007/s11356-016-8214-8).
- [19] G. De Carolis, M. Adamo, G. Pasquariello, D. De Padova, and M. Mossa, “Quantitative characterization of marine oil slick by satellite near-infrared imagery and oil drift modelling: The fun shai hai case study,” *Int. J. Remote Sens.*, vol. 34, pp. 1838–1854, 2013.
- [20] M. Adamo, G. De Carolis, V. De Pasquale, and G. Pasquariello, “Detection and tracking of oil slicks on sun-glittered visible and near infrared satellite imagery,” *Int. J. Remote Sens.*, vol. 30, pp. 6403–6427, 2009.
- [21] E. Armenio, M. Ben Meftah, D. De Padova, F. De Serio, and M. Mossa, “Monitoring systems and numerical models to study coastal sites,” *Sensors J.*, vol. 19, no. 7, 2019, Art. no. 1552, doi: [10.3390/s19071552](https://doi.org/10.3390/s19071552).
- [22] I. Leifer, R. Clark, C. Jones, B. Holt, J. Svejkovsky, and G. Swayse, “Satellite and airborne oil spill remote sensing: State of the art and application to the BP deepwater horizon oil spill,” *Remote Sens. Environ.*, vol. 124, pp. 270–295, 2011.
- [23] P. Tkalich, “A CFD solution of oil spill problems,” *Environ. Model. Softw.*, vol. 21, no. 2, pp. 271–282, 2006, doi: [10.1016/j.envsoft.2004.04.024](https://doi.org/10.1016/j.envsoft.2004.04.024).
- [24] Y. Liu, R. H. Weisberg, C. Hu, and L. Zheng, “Tracking the deepwater horizon oil spill: A modeling perspective,” *EOS Trans. AGU*, vol. 92, no. 6, pp. 45–46, 2011, doi: [10.1029/2011EO060001](https://doi.org/10.1029/2011EO060001).
- [25] Y. Liu, R. H. Weisberg, C. Hu, and L. Zheng, “Trajectory forecast as a rapid response to the deepwater horizon oil spill,” in *Book Monitoring and Modeling the Deepwater Horizon Oil Spill: A Record-Breaking Enterprise (Geophysical Monograph Series)*, vol. 195. Hoboken, NJ, USA: Wiley, 2011, pp. 153–165.
- [26] A. J. Abascal, S. Castanedo, R. Minguez, R. Medina, Y. Liu, and R. H. Weisberg, “Stochastic Lagrangian trajectory modeling of surface drifters deployed during the deepwater horizon oil spill,” in *Proc. 38th AMOP Tech. Seminar Environ. Contamination Response, Environ. Climate Change*, 2015, pp. 71–99.
- [27] B. G. Gautama, N. Longépé, R. Fablet, and G. Mercier, “Assimilative 2-D Lagrangian transport model for the estimation of oil leakage parameters from SAR images: Application to the montara oil spill,” *IEEE J. Sel. Topics Appl. Earth Observ. Remote Sens.*, vol. 9, no. 11, pp. 4962–4969, Nov. 2016, doi: [10.1109/JSTARS.2016.2606110](https://doi.org/10.1109/JSTARS.2016.2606110).
- [28] L. C. Jeznach *et al.*, “Modeling crude oil fate and transport in freshwater,” *Environ. Model. Assessment*, vol. 26, pp. 77–87, 2021.
- [29] Q. A. Dang *et al.*, “Mathematical modeling and numerical algorithms for simulation of oil pollution,” *Environ. Model. Assessment*, vol. 17, pp. 275–288, 2012.
- [30] P. Keramea, K. Spanoudaki, G. Zodiatis, G. Gikas, and G. Sylaios, “Oil spill modeling: A critical review on current trends, perspectives, and challenges,” *J. Mar. Sci. Eng.*, vol. 9, 2021, Art. no. 181, doi: [10.3390/jmse9020181](https://doi.org/10.3390/jmse9020181).
- [31] A. Soussi *et al.*, “An oil spill trajectory model: Validation in the Mediterranean sea,” in *Proc. Int. Symp. Syst. Eng.*, 2019, pp. 1–6, doi: [10.1109/ISSE46696.2019.8984542](https://doi.org/10.1109/ISSE46696.2019.8984542).
- [32] A. Zafirakou, “Oil spill dispersion forecasting models in book monitoring of marine pollution,” in *Proc. IntechOpen*, 2018, pp. 1–20.
- [33] Y. Liu and R. H. Weisberg, “Evaluation of trajectory modeling in different dynamic regions using normalized cumulative Lagrangian separation,” *J. Geophys. Res.*, vol. 116, 2011, Art. no. C09013, doi: [10.1029/2010JC006837](https://doi.org/10.1029/2010JC006837).
- [34] C. Dearden, T. Culmer, and R. Brooke, “Performance measures for validation of oil spill dispersion models based on satellite and coastal data,” *IEEE J. Ocean. Eng.*, vol. 47, no. 1, pp. 126–140, Jan. 2022, doi: [10.1109/JOE.2021.3099562](https://doi.org/10.1109/JOE.2021.3099562).
- [35] S. Magri, M. Quagliatia, P. D. Gaetanoa, T. Vairoab, and B. Fabianob, “Fuel spill after ship collision: Accident scenario modelling for emergency response,” *Chem. Eng. Trans.*, vol. 74, pp. 1363–1368, 2019.
- [36] Jan. 2021. Accessed: Apr. 2, 2020. [Online]. Available: <https://search.asf.alaska.edu/#/>
- [37] A. H. Al-Rabeh, “Estimating surface oil spill transport due to wind in the Arabian gulf,” *Ocean Eng.*, vol. 21, no. 5, pp. 461–465, 1994.

- [38] K. D. Stolzenbach, E. E. Madsen, A. Adams, A. Pollack, and C. Cooper, "A review and evaluation of basic technique for predicting the behaviour of surface oil slicks," Dept. Civil Eng., Massachusetts Inst. Technol., Cambridge, MA, USA, Rep. 22, 1977.
- [39] M. Reed, C. Turned, and A. Odulo, "The role of wind and emulsification in modelling oil spill and surface drifter trajectories," *Spill Sci. Technol. Bull.*, vol. 1, pp. 143–157, 1994.
- [40] M. A. Badri, "Applying genetic algorithm to minimize the oil spill damage and optimize the location of the cleaning vessels," *Indian J. Geo-Mar. Sci.*, vol. 43, no. A, pp. 489–498, Apr. 2014.
- [41] Jan. 2021. Accessed: Sep. 9, 2020. [Online]. Available: <https://cds.climate.copernicus.eu/cdsapp#!/dataset/reanalysis-era5-single-levels?tab=form>
- [42] Jan. 2021. Accessed: Sep. 9, 2020. [Online]. Available: <https://gnome.orr.noaa.gov/goods/winds/NDBC/source>
- [43] Jan. 2021. Accessed: Sep. 9, 2020. [Online]. Available: https://gnome.orr.noaa.gov/goods/currents/SSH/get_data
- [44] R. Nau, "Notes on the random walk model," *Fuqua Sch. Bus.*, vol. 1, pp. 1–19, 2014.
- [45] E. P. Xing, "Factor analysis and state space models," in *Probabilistic Graphical Models*. Spring, 2017, ch. 11, pp. 10–708.
- [46] M. Fingas, "A review of natural dispersion models," *Int. Oil Spill Conf. Proc.*, vol. 2014, pp. 207–224, Jan. 2013, doi: [10.7901/2169-3358-2014-1-285471.1](https://doi.org/10.7901/2169-3358-2014-1-285471.1).
- [47] M. F. Fingas, "Studies on the evaporation of crude oil and petroleum products: I. The relationship between evaporation rate and time," *J. Hazardous Mater.*, vol. 56, no. 3, pp. 227–236, 1997.
- [48] S. Liubartseva, M. Smaoui, G. Coppini, G. Gonzalez, R. Lecci, and I. Federico, "Corsica oil spill, October–November 2018: Fusion of modelling and observations," *Geophys. Res. Abstr.*, vol. 21, 2019, Art. no. EGU2019-3289.
- [49] A. J. Abascal, S. Castanedo, R. Medina, I. J. Losada, and E. Alvarez-Fanjul, "Application of HF radar currents to oil spill modelling," *Mar. Pollut. Bull.*, vol. 58, pp. 238–248, 2009.
- [50] R. H. Weisberg, L. Zheng, and Y. Liu, "On the movement of deepwater horizon oil to northern gulf beaches," *Ocean Model.*, vol. 111, pp. 81–97, 2017.
- [51] Jan. 2021, Accessed: Jan. 1, 2021. [Online]. Available: <https://response.restoration.noaa.gov/oil-and-chemical-spills/oil-spills/response-tools/gnome.html>
- [52] A. S. Dhavalikar and P. C. Choudhari, "Classification of oil spills and look-alikes from SAR images using bag of visual words method of feature extraction," in *Proc. IEEE Int. Geosci. Remote Sens. Symp.*, 2021, pp. 3428–3431, doi: [10.1109/IGARSS47720.2021.9554307](https://doi.org/10.1109/IGARSS47720.2021.9554307).
- [53] M. De Dominicis, N. Pinardi, G. Zodiatis, and R. Archetti, "MEDSLIK-II, a lagrangian marine surface oil spill model for short-term forecasting—Part 2: Numerical simulations and validations," *Geosci. Model Develop.*, vol. 6, pp. 1871–1888, 2013, doi: [10.5194/gmd-6-1871-2013](https://doi.org/10.5194/gmd-6-1871-2013).



Anagha S. Dhavalikar (Student Member, IEEE) received the B.E. degree in electronics from the University of Pune, Pune, India, in 2004, and the M.E. degree in electronics & telecommunication engineering from the University of Mumbai, Mumbai, India, in 2014. She is currently working toward the Ph.D. degree in electronics & telecommunications with the Father Conceicao Rodrigues Institute of Technology, Navi Mumbai, India.

She is currently affiliated with the Electronics & Telecommunication Engineering Department, Vasantadada Patil Pratishthan's College of Engineering & Visual Arts, Mumbai, as an Assistant Professor. She has completed the M.E. thesis with the Development of Automatic Face Detection and Facial Expression Recognition System using Artificial Neuro-Fuzzy Inference System. Her research interests include automatic detection of offshore oil spills using synthetic aperture radar (SAR) images. Her research interests also include image processing with applications to spaceborne SAR data and machine learning for development of ocean remote sensing applications.

Ms. Dhavalikar is a life member of ISTE.



Pranali C. Choudhari received the B.E. degree in electronics and telecommunication engineering from the Pune University, Pune, India, in 2002, the M.Tech. degree in communication and signal processing from IIT, Mumbai, India, in 2009, and the Ph.D. degree in electronics engineering from the Veermata Jijabai Technological Institute, Mumbai, in 2019.

She has more than 20 years of professional experience in Electronics & Telecommunication Engineering. Being passionate about teaching, she began her professional career in 2002 and is an Associate Professor with the Father Conceicao Rodrigues Institute of Technology, Navi Mumbai, India. She has been teaching UG as well as PG course related to Signal Processing, Internet of Things, and Embedded Systems. She has received research grants in the field of biomedical signal processing from the University of Mumbai, Mumbai. She has authored/coauthored around 40 papers in various reputed International Journals and Conferences. She has received 116 citations to her papers. She is a Reviewer for reputed publications like International Journal for Numerical Methods in Biomedical Engineering, Wiley Journals, and IEEE JOURNAL OF BIOMEDICAL AND HEALTH INFORMATICS. She is an approved Teacher for both graduate as well as post graduate with the University of Mumbai. She has also guided 20 projects at undergraduate, nine projects at post graduate level, and three Ph.D. theses. Her research interests include biomedical signal processing, artificial intelligence, image and video processing, Internet of Things, and embedded systems.

Dr. Choudhari is member of professional bodies such as IETE, ISTE, and IIIE.